Catal Lett (2009) 128:111–118
DOI 10.1007/s10562-008-9697-9

Enhanced Catalytic Activity of Ti, V, Mn-Grafted Silica Spheres Towards Epoxidation Reaction

D. P. Das · K. M. Parida

Received: 10 January 2008 / Accepted: 5 February 2008 / Published online: 11 October 2008

Abstract A simple, cost effective and reusable transition metal (M = Ti, V, Mn)-grafted mesoporous silica spheres were synthesized by sol–gel technique and characterized by SXRD, FTIR, UV–Vis DRS, SEM, EDS, BET-surface area, pore volume and average pore diameter. Epoxidation of cyclohexene to cyclohexene oxide over these modified silica spheres using TBHP as oxidant was performed to compare the catalytic activities. Cyclohexene oxide selectivity was recorded to be 87.5% with 72.5% conversion over 8 wt% Ti-grafted silica spheres in comparison to V and Mn-grafted catalysts.

Keywords Transition metal grafted · Cyclohexene · Epoxidation · TBHP · Cyclohexene oxide

1 Introduction

Cyclohexene oxide (epoxycyclohexane) is a useful monomer in polymerisation and coating industries. It is used in the synthesis of alicyclic target materials including pesticides, pharmaceuticals, perfumery and dye stuffs. It is used as monomer in photopolymerisation with CO to yield aromatic polycarbonates. In industries it is used for the production of adipic acid. The direct oxidation of hydrocarbons to form epoxides is one of the most important reactions because of its applications in organic synthesis, food, agrochemicals and pharmaceutical industries [1, 2]. Till date the catalysts containing Ti and Si are known to be the most powerful heterogeneous epoxidation catalysts [3]. A number of investigations have been made on titania-silica mixed oxide system [4], Ti-silica hollow spheres [5], Ti-SBA-15 [6], oxovanadium (IV) based co-ordination polymers [7], Ti-containing zeolites [8] towards epoxidation of cyclic alkenes. Schmidt et al. [8] have reported 90% cyclohexene oxide selectivity taking methanol as solvent, hydrogen peroxide as oxidant over Ti-zeolite. Mendez et al. [9] reported 51.5 (100% epoxide selectivity), 146 (38.5% 2-cyclohexen-1-ol and 61.5% 2-cyclohexen-1-one selectivity) and 44.4 h^{-1} TOF (51.4% 2-cyclohexen-1-ol and 49.6% 2-cyclohexen-1-one selectivity), respectively over TiO_2/SiO_2, V_2O_5/SiO_2 and Nb_2O_5/SiO_2 taking TBHP as oxidant. Chiker et al. [10] have investigated the selective oxidation of cyclohexene, styrene, limonene, α-pinene taking Ti-SBA15 as catalyst, TBHP as oxidant and acetonitrile as solvent. They reported the cyclohexene conversion to be 71% with 100% epoxide selectivity. Ingold et al. [11] reported cyclohexene epoxide selectivity 0.28–21 eq. taking different solvents 2-propanol-acetonitrile, respectively in 24 h TBHP as oxidant over Ti-MCM41 as catalyst.

There is restriction in the use of hydrogen peroxide as oxidant in the epoxidation reaction due to co-production of water. Most transition metal catalysts are very sensitive to water which causes them to leach their active metallic sites. In case of a stable catalyst, water has a serious retarding effect on epoxidation reaction, making the search for new environmentally friendly, effective epoxidation catalysts a challenging one. Cyclohexene epoxidation over an efficient and reusable Ti, V and Mn-grafted silica spheres, using TBHP as oxidant and toluene as solvent was studied (Scheme 1). The correlation between the transition metal content of the catalyst and the catalytic activity was also studied to clarify the origin of the catalysis.

D. P. Das (✉) · K. M. Parida (✉)
Colloids & Materials Chemistry Department, Institute of Minerals & Materials Technology (CSIR), Bhubaneswar 751013, Orissa, India
e-mail: das_diptiprakasini@rediffmail.com

K. M. Parida
e-mail: kmparida@yahoo.com

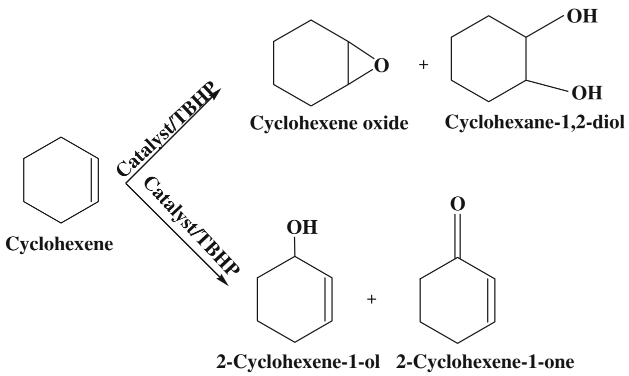

Scheme 1 Cyclohexene epoxidation over transition metal-grafted silica spheres

2 Materials and Methods

2.1 Materials

Sodium metalsilicate ($Na_2SiO_3{\cdot}9H_2O$) (CDH (P) Ltd.), cetyltrimethylammonium bromide (CTAB) ($C_{16}H_{33}(CH_3)_2N^+Br^-$) (S.D. fine chemicals), 2-propanol (S.D. fine chemicals, 99.5%), Ti (VI) isopropoxide (Sigma–Aldrich, 97%), Vanadyl sulfate (Across Organics, 17–23% V), Mn (II) acetate (BDH, 99%).

2.2 Synthesis of Ti, V, Mn-Grafted Silica Spheres

2.2.1 Silica Sphere

Spherical mesoporous silica was prepared by using CTAB as surfactant and propanol as cosurfactant. Following the procedure reported by Das et al. [12], a mixture of propanol and CTAB (10.76 mmol) in the molar ratio 8.5:1 was dissolved in water. $Na_2SiO_3{\cdot}9H_2O$ (4 g) was then added (the total volume of the mixed solution was kept constant at 140 mL). It was stirred for around 30 min to get a clear solution. Then 10 mL of ethyl acetate was added to the clear solution. This clear mixture was kept under stirring condition for 5 h at room temperature. After hydrolysis, the mixture was kept at 80 °C for 72 h in an air oven. The resulting solid was recovered by filtration, washed with distilled water and ethanol. Then it was dried at 80 °C in an air oven. The surfactants were removed by calcination at 540 °C for 6 h. This is designated as S.

2.2.2 Ti–SiO$_2$

Ti–SiO_2 was prepared by hydrolysis of titanium tetraisopropoxide (TTIP) into silica sphere via a sol–gel method (Post synthesis). In a typical synthesis, 1 g of the above mentioned silica sphere was stirred in 10 mL of 2-propanol for 1 h. A required amount of TTIP in 2-propanol (volume ratio TTIP:2-propanol of 1:10) was added drop wise to the suspension with stirring for 45 min, the resulting mixture was slowly added water (TTIP:Water volume ratio = 1:10) to cause the hydrolysis of TTIP. The stirring was maintained for 2 h to hydrolyse TTIP completely. The as-synthesised materials were recovered by centrifugation, rinsed with deionised water, ethanol and dried overnight and calcined at 540 °C for 6 h. The samples are designated as TS2-TS20 depending on the wt% loading of Ti on silica spheres.

2.2.3 V–SiO$_2$ and Mn–SiO$_2$

V- and Mn-grafted silica sphere were prepared by using CTAB as surfactant and propanol as cosurfactant (in situ method). A mixture of CTAB (10.76 mmol) and propanol (the molar ratio of propanol to CTAB = 8.5:1) was dissolved in water. $Na_2SiO_3{\cdot}9H_2O$ (4 g) was then added (the total volume of the mixed solution was kept constant at 140 mL). A required amount of vanadyl sulfate/Mn (II) acetate as the source of vanadium/manganese was added before addition of sodium silicate. It was stirred for around 30 min to get a clear solution. Then 10 mL of ethyl acetate was added to the clear solution. This clear mixture was kept under stirring condition for 5 h at room temperature. After hydrolysis, the mixture was kept at 80 °C for 72 h in an air oven. The resulting solid was recovered by filtration, washed with distilled water followed by ethanol. Then it was dried at 80 °C. The surfactants were removed by calcination at 540 °C for 6 h. These samples are symbolized as VS2, VS4, MnS2, MnS4 and so on.

2.3 Characterization

The samples were characterized by SXRD, SEM-EDS, FTIR, BET-surface area, and N_2 adsorption-desorption studies. SXRD patterns of powdered samples were taken on Rigaku Miniflex diffractometer in the 2θ range from 1 to 5° at a rate of 0.5°/min in steps of 0.01° (operating at 30 kV and 15 mA) using Cu-Kα radiation. N_2 adsorption-desorption studies were carried out by ASAP 2020 (Micromeritics) instrument at liquid nitrogen temperature (−196 °C). Prior to analysis, the particles were subjected to vacuum (10^{-6} torr) at 250 °C to ensure a clean surface. Surface areas were calculated with Brunauer-Emmett-Teller (BET) method using the adsorption data within the *p/po* range from 0.05 to 0.33. The pore volumes were taken at a relative pressure *p/po* of 0.95. Pore size distributions were analysed using Barrett-Joyner-Halenda (BJH) model. Scanning electron microscopy (SEM) images were taken on a Hitachi S-3400N scanning electron microscope. Quantitative EDS microanalyses were made in an SEM (Hitachi S-3400N). The SEM operating condition was

15 kV. The samples were sputtered with a thin film of gold. FTIR spectra were recorded on Varian FTIR spectrophotometer (FTS 800) in the range from 4000 to 400 cm^{-1}. Each spectrum was recorded at 4 cm^{-1} resolution with 30 scans. UV–Vis spectra were taken with a Varian Cary 1E spectrophotometer equipped with a diffuse-reflectance accessory in the region 200–800 nm.

2.4 Catalytic Activity Evaluation

The cyclohexene epoxidation over Ti-, V-, Mn-grafted SiO_2 sphere was carried out under reflux, using reaction mixture containing 10 mmol cyclohexene, 20 mmol TBHP and 20 mg of freshly activated catalyst in toluene for 5 h. The products were analysed by Shimadzu gas chromatography (GC 2010) in a ZBWAX capillary column.

3 Results and Discussion

3.1 Characterisation of Catalysts

The dispersed microspheres were distinctly identified by scanning electron microscope (SEM and EDS, Fig. 1a–c).

Table 1 shows an increase in the BET surface area of the catalysts up to 4 wt% metal loading and thereafter decreases along with the average pore diameter and pore volume due to pore blockage (covering effect). N_2 adsorption desorption studies reveal that all the catalysts are mesoporous in character showing Type IV isotherm and H1 hysteresis loop (Fig. 2a–c).

Examination of these catalysts by low angle X-ray diffraction studies reveal that the hexagonal character of the silica spheres is slowly destroyed with increase (>4 wt%)

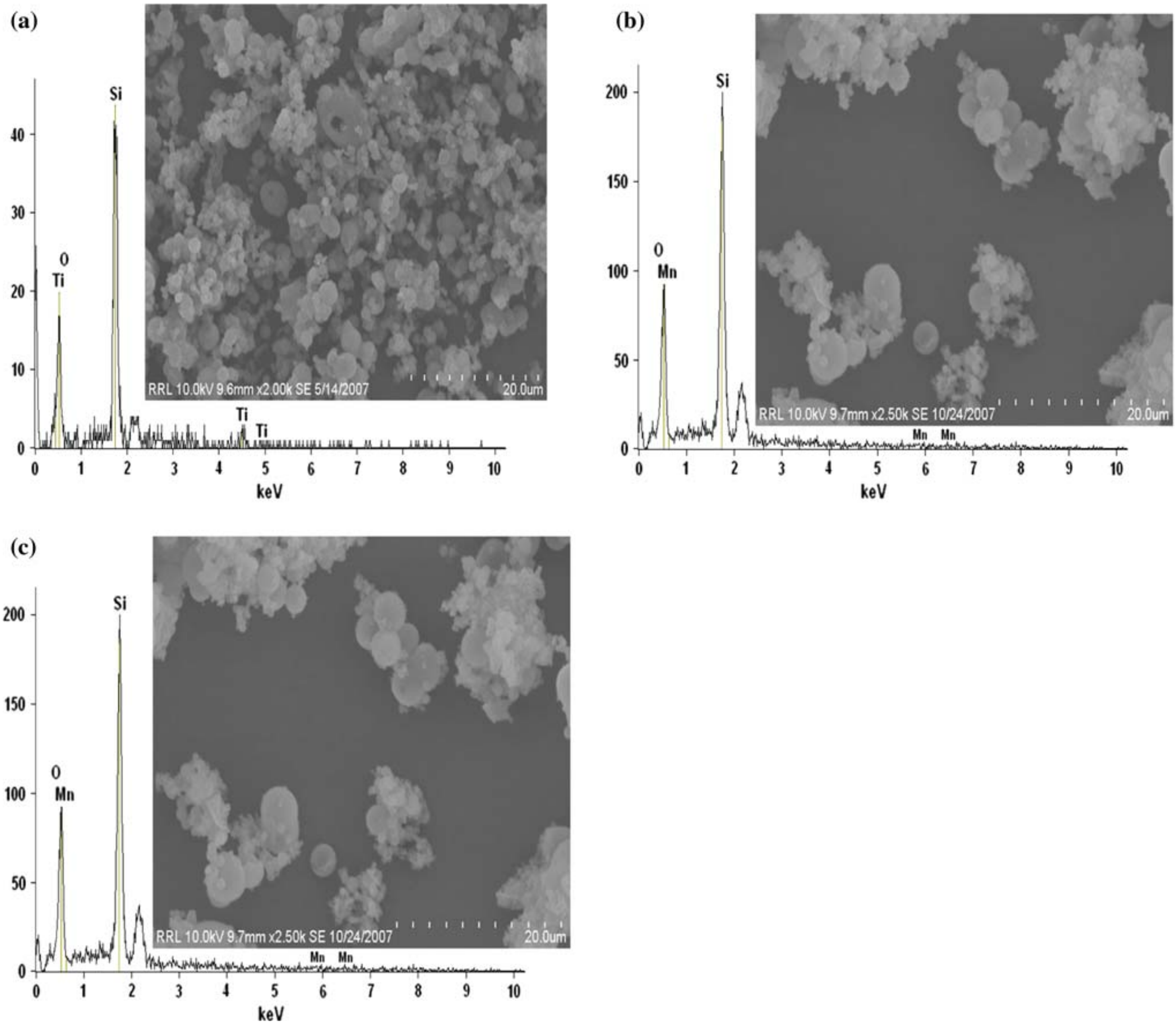

Fig. 1 SEM and EDS micrographs. **a** TS4. **b** VS4. **c** MnS4

Table 1 Textural properties of the materials

Samples	Surface area ($m^2\ g^{-1}$)	Pore volume ($cm^3\ g^{-1}$)	APD[a] (Å)
S	971	2.12	26
TS2	837.75	1.57	24.8
TS4	950.71	1.64	26.4
TS8	946.2	1.49	25.26
TS10	857.29	1.24	24.8
TS15	805.45	1.17	24.4
TS20	756.9	1.16	22.66
VS2	936.17	1.49	23.2
VS4	946.7	1.63	25.0
VS8	900.16	1.22	20.6
VS10	832.5	1.15	19.2
MnS2	822.9	1.4	24.8
MnS4	875.32	1.62	26.3
MnS8	860.59	1.35	20.5
MnS10	840.34	1.1	18.32

[a] *APD* Average pore diameter (determined using BJH analysis)

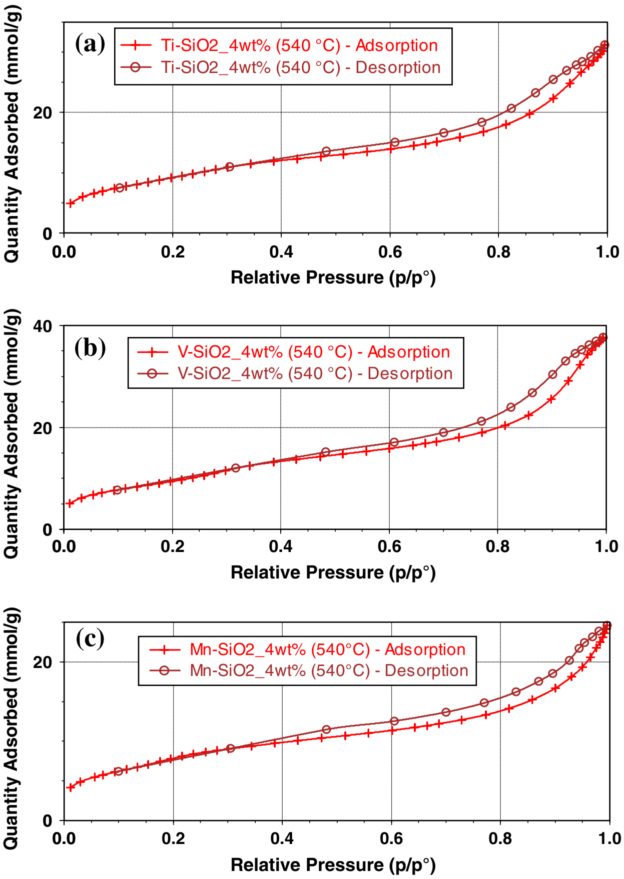

Fig. 2 N_2 ads–des isotherm. **a** 4 wt% Ti. **b** 4 wt% V. **c** 4 wt% Mn-grafted silica spheres

in transition metal loading (see Fig. 3a–c). This may possibly be due to the changes in chemical composition by addition certain amount of elements with larger ionic radius compared to silicon. The detailed explanation is given below.

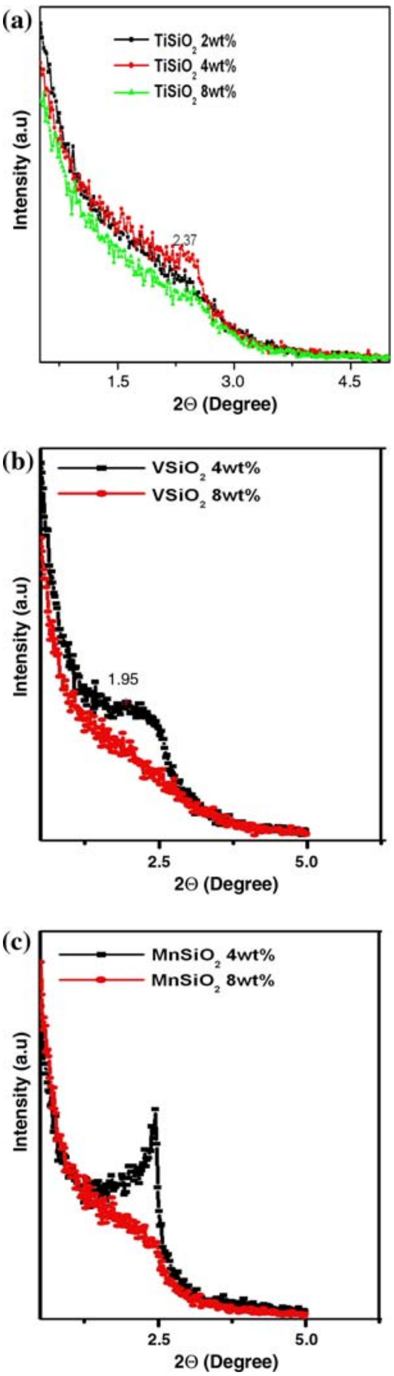

Fig. 3 Low angle XRD patterns. **a** Ti. **b** V. **c** Mn-grafted silica spheres

Infrared spectroscopy has been used extensively for the characterization of transition metal grafted catalysts. The broad bands at around 3500 cm^{-1} may be attributed to surface silanols and adsorbed water molecules, while deformational vibration of adsorbed molecules cause the absorption bands at 1649 cm^{-1} [13]. The substitution of

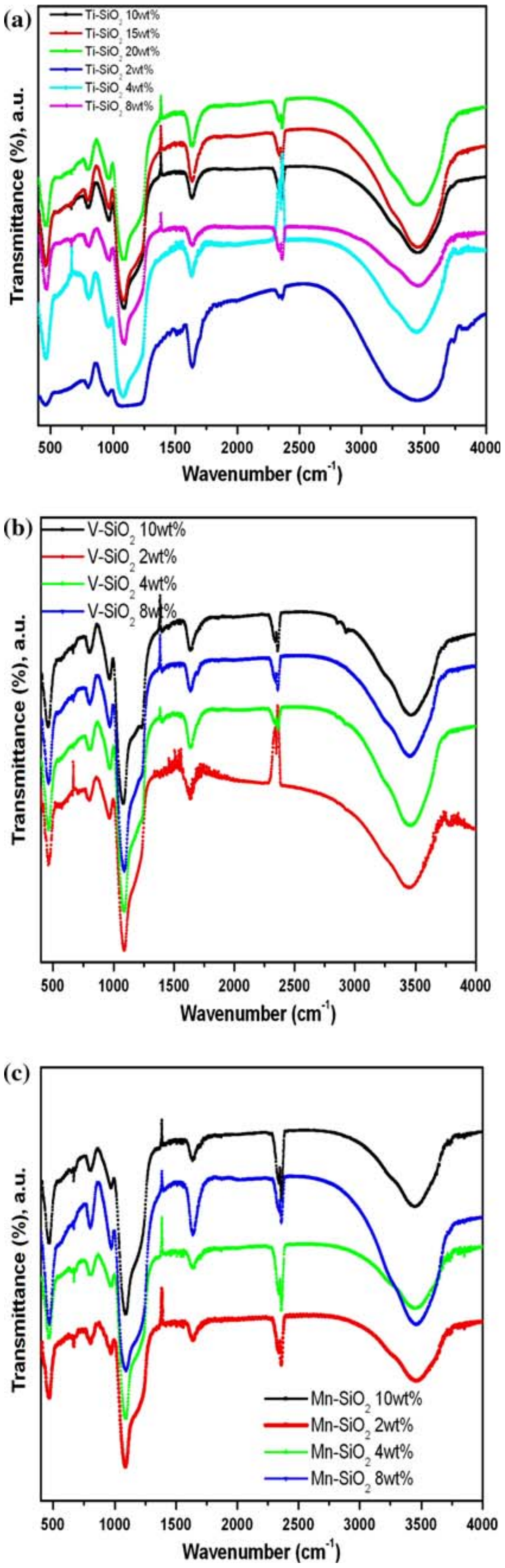

Fig. 4 FTIR spectra. **a** Ti. **b** V. **c** Mn-grafted silica spheres using KBr wafers

silicon by V, Mn causes a shift of the lattice vibration bands to lower wavenumbers (Fig. 4b, c). Compared to neat silica spheres, the wavenumber of antisymmetric Si–O–Si vibration band of VS and MnS samples decreases to 1091 and 1095 cm^{-1}, respectively (Fig. 4b, c). These shifts should be due to the increase in mean Si–O distance in the walls caused by the substitution of small silicon (radius 54 pm) by larger size V^{5+} (radius 68 pm), Mn^{3+} (radius 75.3 pm) [14]. In case of Ti-grafted silica sphere a band was observed at 974 cm^{-1} due to modification of silanol groups (Fig. 4a) [15]. Additionally, an adsorption band at 975 cm^{-1} was observed in case of VS and MnS assigned to a stretching vibration of Si–O–M^{+} linkage. This is generally considered to be a proof of incorporation of the heteroatom into the framework as reported by Selvaraj and co-workers [16, 17].

Figure 5 shows the UV–Vis spectra of 4 wt% Ti-, V- and Mn-grafted silica spheres. TS4 sample shows a band at 223–241 nm, attributed to distorted tetrahedral Ti-species in mesoporous structure which is in good agreement with Bhaumik and Tatsumi [18]. The electronic spectra of VS4, displays a broad absorption peak centered at 254 nm and a shoulder at 366 nm. This is a strong evidence of uniform distribution of vanadium species in the framework of silica sphere. The former absorption band attributes towards V^{+5} species inside the hexagonal wall and the latter towards V^{+5} on the surface [19]. It was observed that Mn^{+2} and Mn^{+3} species as coexisting, may be coordinated with Si (IV) sphere support by distorted octahedral and tetrahedral environments, respectively.

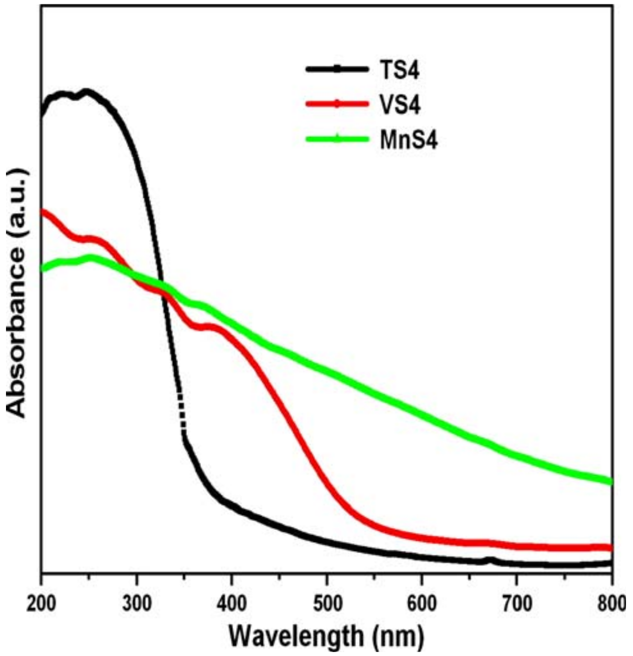

Fig. 5 UV–Vis DRS spectra of TS4, VS4 and MnS4

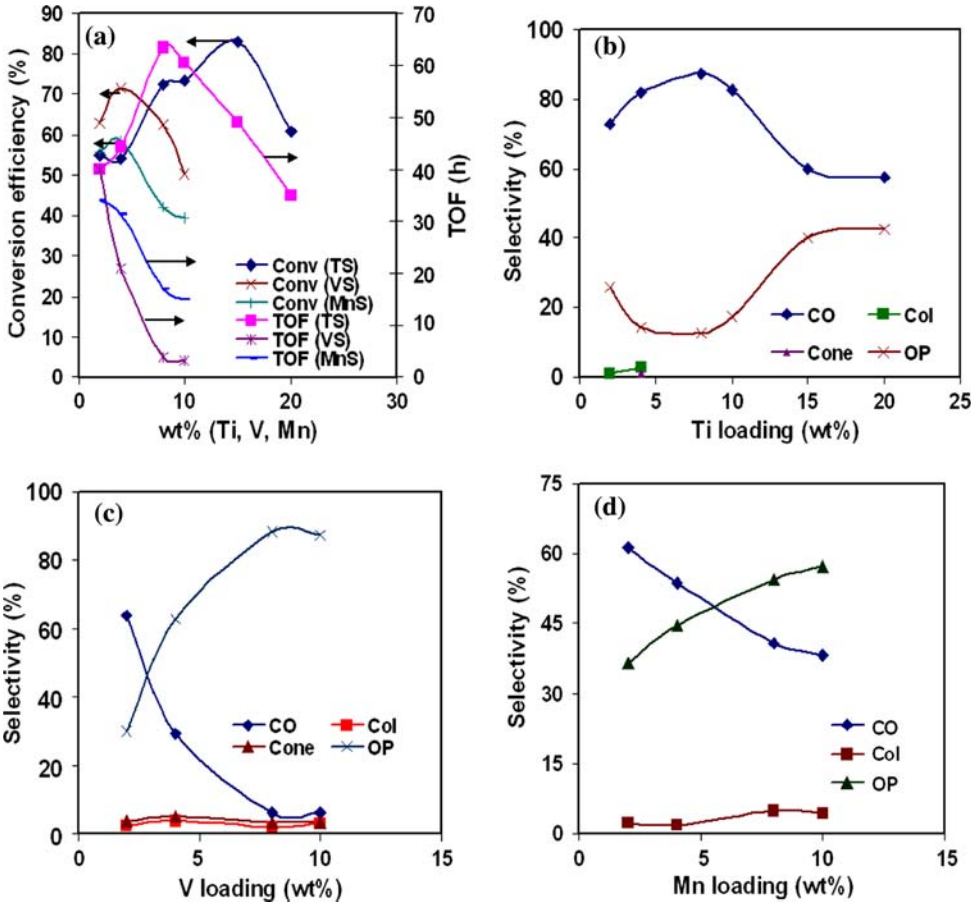

Fig. 6 Epoxidation of cyclohexene by anhydrous TBHP. **a** Conversion efficiency and TOF (h), selectivity (%) over **b** Ti, **c** V, and **d** Mn-planted silica spheres [CO cyclohexene oxide, Col 2-cyclohexene-1-ol, Cone 2-cyclohexene-1-one, OP other products]

3.2 Epoxidation of Cyclohexene

Results on epoxidation of cyclohexene over Ti, V, Mn-grafted silica spheres were presented in Fig. 6a. In an attempt to understand the promotional effect of transitional metal grafting onto silica sphere support, we have found that the size of the metal grafted to the support contributes towards the activity. This could be the possible reason for high activity and selectivity of Ti-grafted silica spheres towards cyclohexene oxide formation (see Fig. 1a–c). The results in Fig. 6a–d reveal the following important informations:

(1) Among the transition metal oxide (in different wt%) supported mesoporous silica spheres, TS8 showed the best performance (Fig. 6b) i.e. the highest cyclohexene oxide selectivity (87.5%) and TOF[1] (63.5 h^{-1}). This is mainly due to the fact that Ti-species can replace more no of Si–OH groups which are considered to be Bronsted acid sites producing active Lewis acidic centers compared to Mn and V species [21].

(2) Lowest cyclohexene conversion was observed MnS10 (39.4%) as compared to VS8 (62.6%). But TOF of both the catalysts were observed to be 15.1 and 3.9 h^{-1}, respectively.

(3) Among the three series of transition metal oxide supported silica, Ti-grafted silica sphere showed a good performance in epoxidation of cyclohexene. However, they differed in their cyclohexene conversion activity and selectivity for the formation of oxirane. Also TS4–TS10 showed higher cyclohexene oxide selectivity. The others like VS2 and MnS2 also showed good epoxide selectivity.

(4) The transition metal-grafted silica showed the following order for their performance in the epoxidation (the values in brackets show cyclohexene oxide selectivity): TS8 (87.5%) > TS10 (82.5%) > TS4 (81.9%) $\gg$ TS2 (72.9%) > VS2 (63.8%) > MnS2 (61.2%) > TS15 (60.0%) > TS20 (57.4%) > MnS4 (53.7%) > MnS8 (40.7%) > MnS10 (38.2%) > VS4 (29.3%) $\gg$ VS8 (6.2%) > VS10 (6.1%).

Although not much reports have been published on epoxidation of cyclohexene, our results are quite comparable to that of oxovanadium (IV) based coordination polymers using TBHP [7] and amine modified titania-silica

---

[1] TOF: Defined as mmols of cyclohexene oxide formed per gram of catalyst per hour as calculated by Choudhary et al. [20].

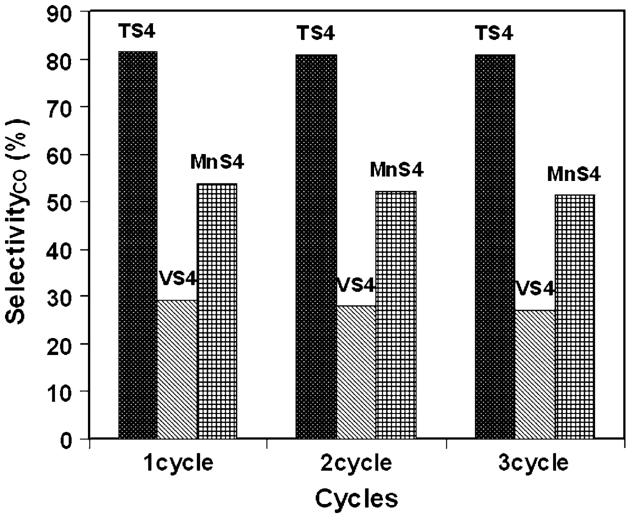

Fig. 7 Catalytic performances of catalysts TS4, VS4 and MnS4 after recycling

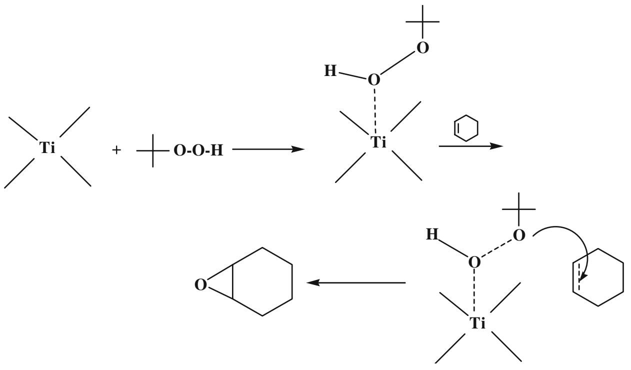

Scheme 2 Possible mechanism for cyclohexene epoxidation through peroxometallic route over Ti-grafted silica sphere

mixed oxides using H_2O_2 [4]. The extra conversion of TBHP is due to its decomposition over the catalyst (with the evolution of oxygen) according to the reaction (1):

$$(CH_3)_3COOH \rightarrow (CH_3)_3COH + 0.5O_2 \tag{1}$$

Based on the key intermediate involved in the oxygen transfer step, the metal catalyzed oxidations can be divided into two categories [22]. The first one involves a peroxometal, while the second one involves an oxometal pathway. Molybdenum, vanadium and titanium catalyzed epoxidations followed peroxometal pathway [23, 24]. Oxometal species, on the other hand, are generally accepted as the reactive intermediaries in catalytic epoxidation with selenium [25], ruthenium [26], osmium [27] and chromium [28]. The present work followed peroxometallic route (Scheme 2). The conversion of cyclohexene to cyclohexene oxide can be explained by the formation of oxygen donating metal-peroxo complexes, arising from the attack of hydroperoxide on metallic centers [29].

Although cyclohexene conversion was found to be more in case of V-grafted silica but the selectivity towards the formation of cyclohexene oxide is more in case of Mn-grafted silica. A serious leaching of V species was also observed at higher V-loading as compared to Mn, which was observed to be very stable in silica framework. This

Table 2 Comparison of the present work with the literature

Entries	Catalyst	Substrate	Conversion (%)	Selectivity (epoxide)	References
1	Tetra-*n*-butyl-ammonium salt of $[\gamma\text{-}1,2\text{-}H_2SiV_2W_{10}O_{40}]^{4-}$	Cyclohexene	–	99	[31]
		Styrene (H_2O_2 as oxidant), acetonitrile and *t*-butyl alcohol (1:1) as solvent, 20 °C, 24 h, 1.67 nM catalyst	–	99	
2	Oxovanadium (IV) based coordination polymers	Cyclohexene	98	45	[7]
		Styrene	68.5	23	
		trans-Stilbene (TBHP as oxidant), acetonitrile as solvent, 75 °C, 6 h, 0.015 g of catalyst	33	6	
3	Alkaline earth and rare earth oxide	Styrene (TBHP as oxidant), benzene as solvent, 82–83 °C, 3 h, 0.1 g catalyst	0.9–40.7	4.1–78.7	[20]
4	Chiral manganese (III) salen complexes functionalized hexagonal mesoporous silica	Styrene (*m*-chloroperoxy benzoic acid as oxidant with *N*-methylmorpholine as co-oxidant, dichloromethane as solvent, 0 °C, 1 h, 0.1 g of catalyst	99	–	[32]
5	Mg/Al hydrotalcite	Styrene (H_2O_2 as oxidant), acetone as solvent, 50 °C, 2 h, 0.5 g of catalyst	97	99.7	[33]
6	Au/TiO_2	Styrene (TBHP as oxidant), benzene as solvent, 82–83 °C, 3 h, 0.1 g of catalyst	60	50	[34]
7	Amine modified TiO_2–SiO_2	Cyclohexene (H_2O_2 as oxidant), toluene as solvent, 90 °C, 2 h, 0.07 g catalyst	46	70.5	[4]

observation was in good agreement with Zhang et al. [30] who investigated the epoxidation of styrene and stilbene in presence of V- and Mn-grafted MCM-41 taking TBHP as oxidant. Further work is needed to understand the mechanism of this epoxidation process. The above discussed catalysts are comparable to other supported catalysts (see Table 2).

Ti-grafted silica sphere was recycled three times without slightest loss in activity and selectivity towards cyclohexene oxide. In case of V- and Mn-grafted samples the activity was decreased slowly with increase in the no of cycles (Fig. 7). This means the structure of active centers is maintained from one cycle to another. Moreover, leaching of catalytically active species can be excluded i.e. a clear solution was observed in presence of TBHP and cyclohexene.

4 Conclusions

Transition metal (M = Ti, V, Mn)-grafted silica spheres are active and environmentally friendly in terms of easy separation, reusability and nontoxicity for the epoxidation of cyclohexene under toluene medium using TBHP as oxidant. Among the three series of transition metal oxide supported silica, Ti-grafted silica spheres showed a good performance in epoxidation of cyclohexene. The activity and selectivity of the catalysts depends on the size as well as the metal loading to the support. The supported catalysts with 4 wt% metal grafting can be recycled three times without loss in activity and selectivity. However, in case of VS4 and MnS4, 1–2% the decrease in selectivity towards cyclohexene oxide was observed after each cycle.

Acknowledgments Authors are very much thankful to Prof. B. K. Mishra, Director, IMMT, Bhubaneswar for his kind support and cooperation and Dr. Nandini Devi, NCL, Pune for doing SXRD analyses. One of the authors DPD is very much thankful to CSIR, New Delhi for a Research Associateship. The financial support from DST, Govt. of India is greatly acknowledged.

References

1. Dusi M, Mallat T, Baiker A (2000) Catal Rev Sci Eng 42:213
2. Gao J, Chen Y, Hau B, Feng Z, Li C, Zhou N, Gao S, Xi Z (2004) J Mol Catal A Chem 210:197
3. Gao XT, Wachs IE (1999) Catal Today 51:233
4. Samantaray SK, Parida KM (2005) Catal Commun 6:578
5. Bala M, Li WJ, Du P, Mul G, Moulijn JA, Coppens M-O (2006) Catal Lett 109:207
6. Chiker F, Nogier JPh, Launay F, Bonardet JL (2003) Appl Catal A Gen 243:309
7. Maurya MR, Kumar A (2006) J Mol Catal A Chem 250:190
8. Schmidt I, Krogh A, Wienberg K, Carlsson A, Brorson M, Jacobsen CJH (2000) J Chem Soc Chem Commun 2157
9. Mendez SM, Henriquez Y, Dominguez O, D'Ornelas L, Krentzien H (2006) J Mol Catal A Chem 252:226
10. Chiker F, Nogier JPh, Launay F, Bonardet JL (2006) Appl Catal A Gen 243:309
11. Ingold KU, Snelgrove DW, MacFaul PA, Oldroyd RD, Thomas JM (1997) Catal Lett 48:21
12. Das DP, Parida KM, Mishra BK (2007) Mater Lett 61:3942
13. Kiseler AV, Lygin VI (1992) Infrared spectra of surface compounds and adsorbed substances. Nauka, Moscow (in Russian)
14. Shannon RD, Prewitt CT (1970) Acta Crystallogr B 26:1046
15. Boccuti MR, Rao KM, Zecchina A, Leofanti G, Petrini G (1989) Stud Surf Sci Catal 48:133
16. Selvaraj M, Min BR, Shul YG, Lee TG (2004) Micropor Mesopor Mater 74:81
17. Selvaraj M, Lee TG (2005) Micropor Mesopor Mater 85:39
18. Bhaumik A, Tatsumi T (2000) J Catal 189:31
19. Luan Z, Xue J, He H, Klinowski J, Kevan L (1996) J Phys Chem 199:19595
20. Choudhary VR, Jha R, Jena P (2006) Green Chem 8:689
21. Sheldon RA (1980) J Mol Catal 7:107
22. Sheldon RA, Dakka J (1994) Catal Today 19:215
23. Mimoun H, Mignard M, Brechot P, Saussine L (1986) J Am Chem Soc 108:3711
24. Mimoun H (1987) Catal Today 1:281
25. Umbreit MA, Sharpless KB (1977) J Am Chem Soc 99:5526
26. Che C-M (1995) Pure Appl Chem 2:225
27. Lohray BB, Bushan V, Kumar RK (1994) J Org Chem 59:1375
28. Muzart J (1992) Chem Rev 92:113
29. Barker CM, Gleeson D, Kaltsoyannis N, Catlow CRA, Sankar G, Thomas JM (2002) Phys Chem Chem Phys 4:1228
30. Zhang Q, Wang Y, Itsuki S, Shishido T, Takehira K (2002) J Mol Catal A Chem 188:189
31. Mizuno N, Nakagawa Y, Yamaguchi K (2006) J Mol Catal A Chem 251:286
32. Silva AR, Wilson K, Clark JH, Freire C (2006) Micropor Mesopor Mater 91:128
33. Kirm I, Medina F, Rodriguez X, Cesteros Y, Salagre P, Sueiras J (2004) Appl Catal A Gen 272:175
34. Patil NS, Uphade BS, Jana P, Sonawane RS, Bhargava SK, Choudhary VR (2004) Catal Lett 94:89